Supporting Information

An Ion-Conductive Honeycomb Hydrogel with Triple Network Structures for 3D Tactile Sensing and Interaction

Jiaxin Huang [a] [b], Yuanyuan Hou [b], Xiongjun Deng [b], Muhammad Arshad [b], Yaser E. Greish [c], Yanlong Tai * [b], Shanshan Zhu * [b], Da-Zhu Chen * [a]

[a] Shenzhen Key Laboratory of Polymer Science and Technology, Guangdong Research Center for Interfacial Engineering of Functional Materials, College of Materials Science and Engineering, Shenzhen University, Shenzhen, 518055, China

[b] CAS Key Laboratory of Human-Machine Intelligence-Synergy Systems, Shenzhen Institutes of Advanced Technology, Chinese Academy of Sciences, Shenzhen, 518055, China

[c] Department of Chemistry, National Water and Energy Center, UAE University, Al-Ain 15551, United Arab Emirates.

*** Corresponding e-mail: dzchen@szu.edu.cn (D. Z. Chen), ss.zhu1@siat.ac.cn （S. S. Zhu), yl.tai@siat.ac.cn (Y. T. Tai),**

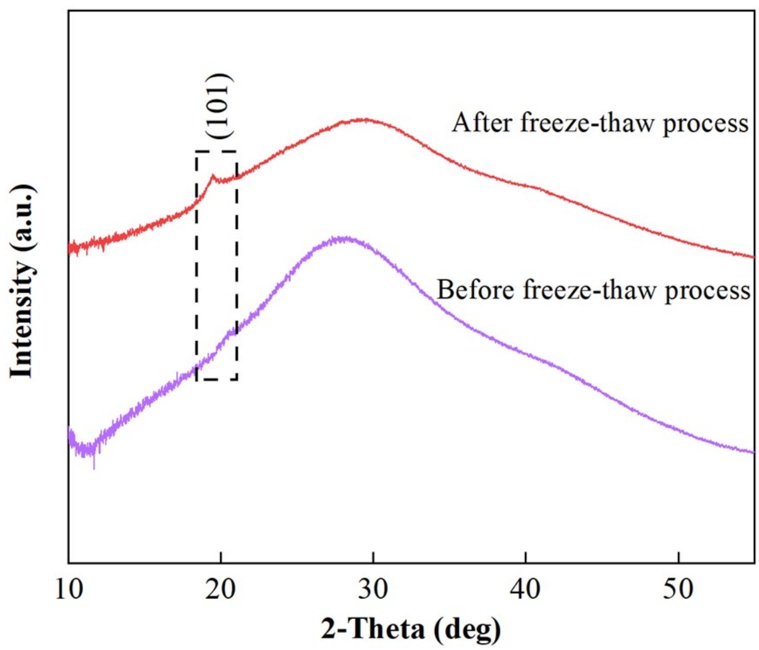

Fig. S1. XRD patterns of P/P/A hydrogel before and after freeze-thaw treatment.

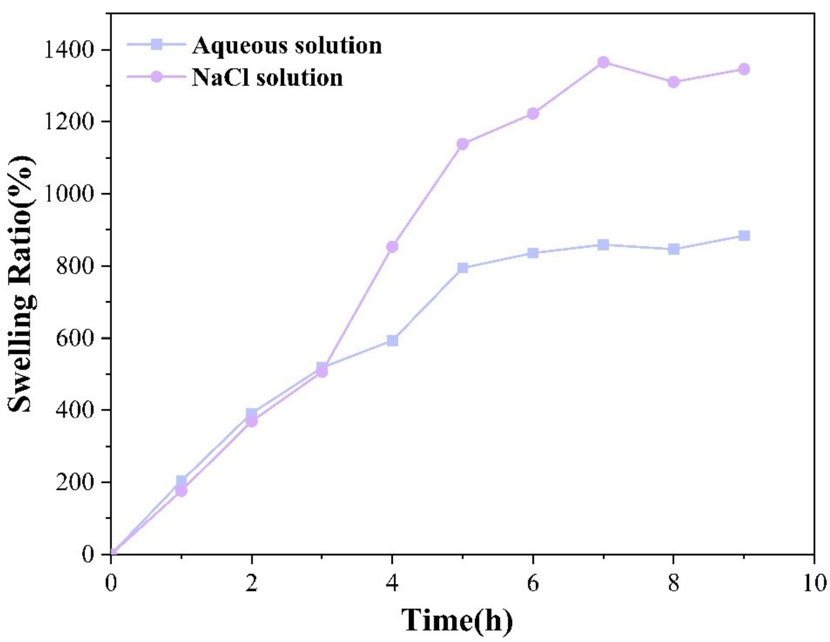

Fig. S2. Swelling rate of P/P/A-NaCl hydrogel in aqueous solution and NaCl solution environments.

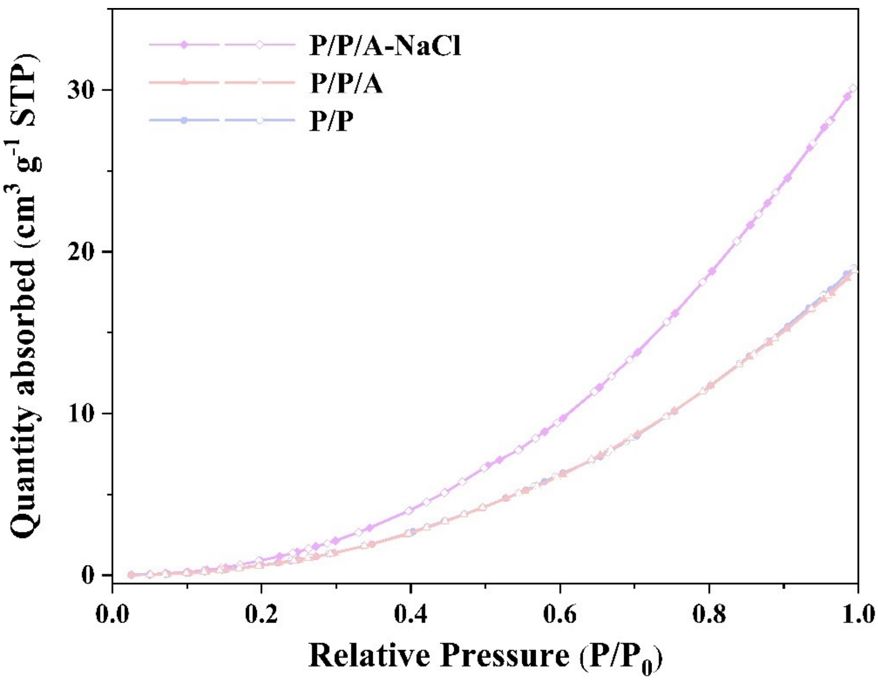

Fig. S3. The nitrogen adsorption and desorption diagrams of different composite hydrogels.

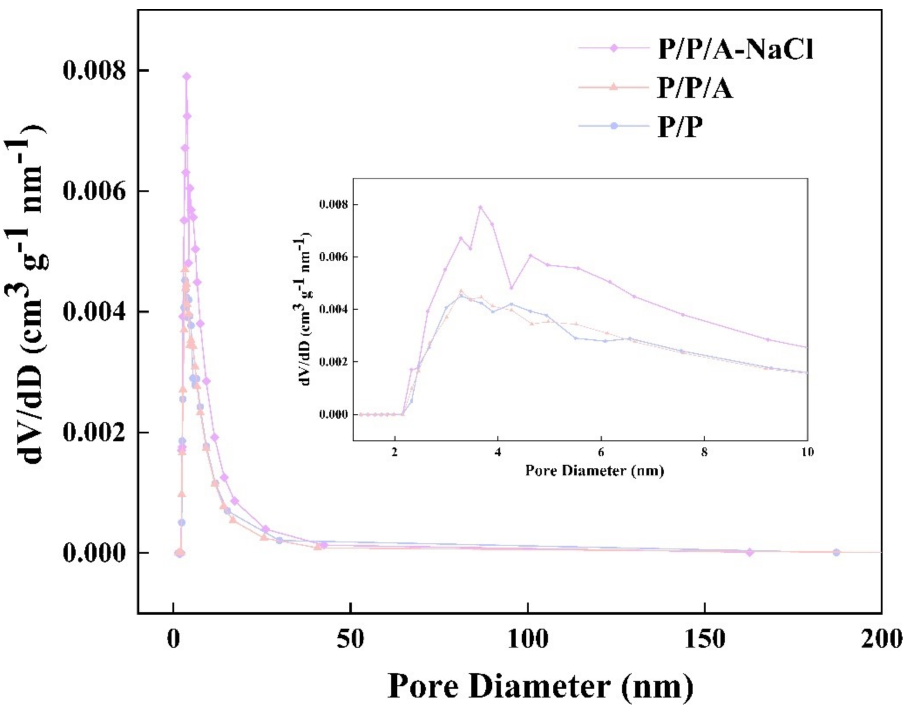

Fig. S4. The BJH pore size distribution of composite hydrogels with microporous structure. The inset shows an enlarged view of the pore size distribution in the 1–10 nm range.

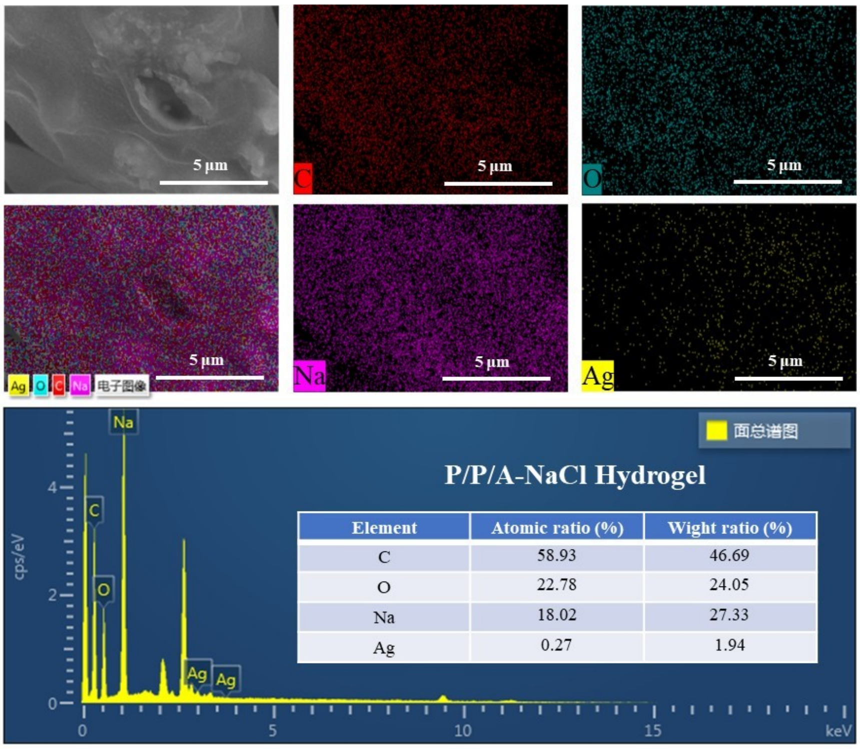

Fig. S5. The EDS spectrum of P/P/A-NaCl hydrogel after freeze-drying.

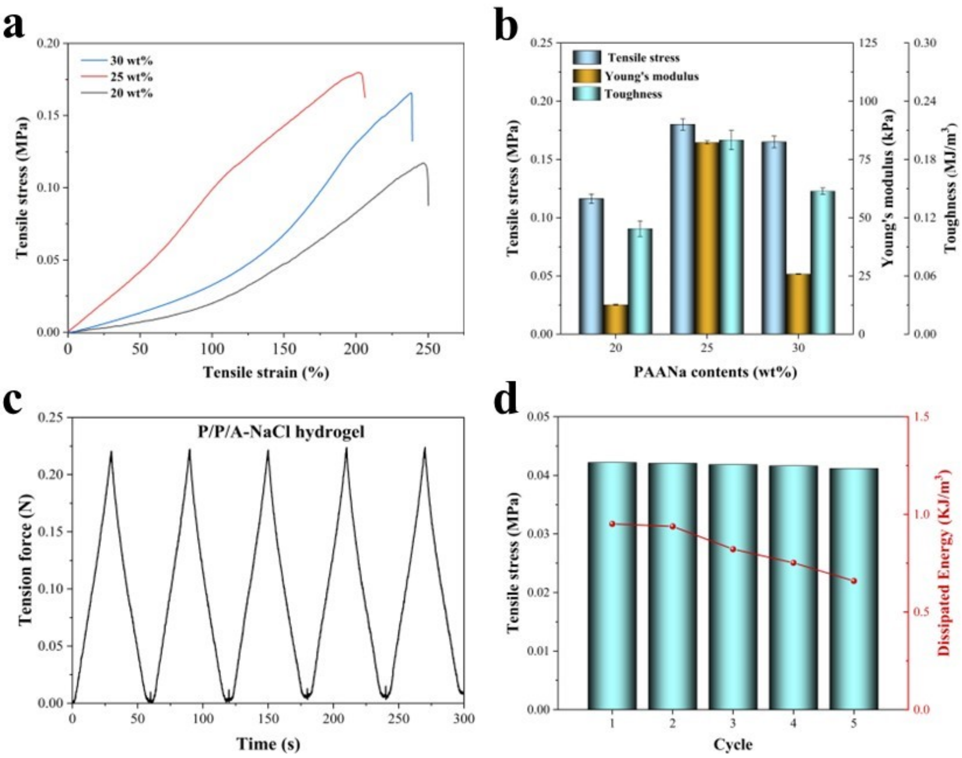

Fig. S6. (a) The tensile stress-strain curves and (b) comparison of tensile stress, Young's modulus, and toughness for P/P Hydrogels with different PAANa contents. (c) The force-time curve and (d) tensile stress value, as well as energy dissipation diagram of P/P/A-NaCl hydrogel for stretching cycle.

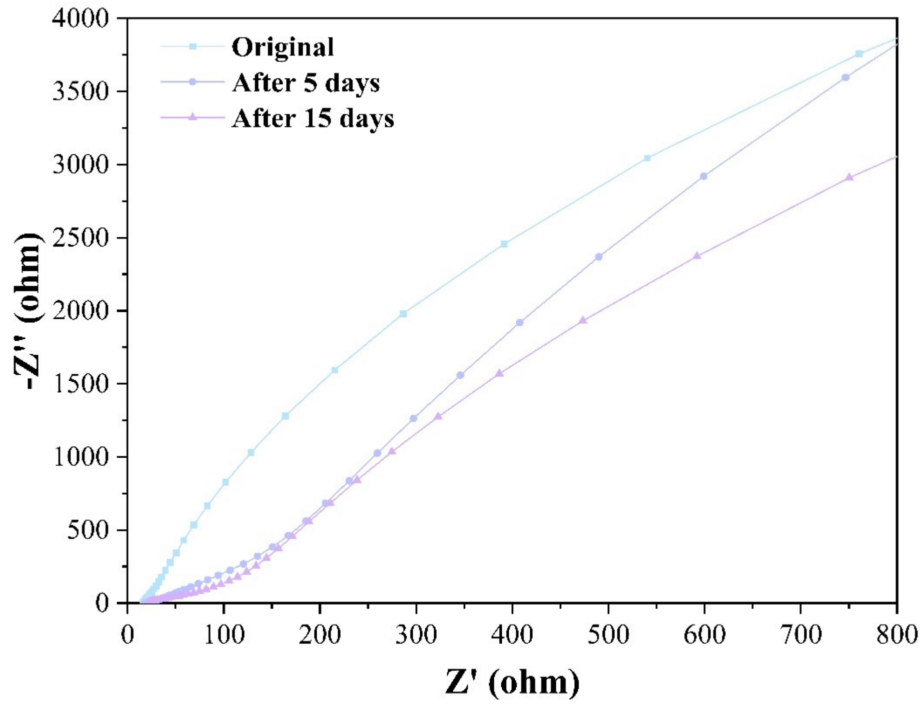

Fig. S7. P/P/A-NaCl hydrogel and its Nyquist curves after 5 days and 15 days.

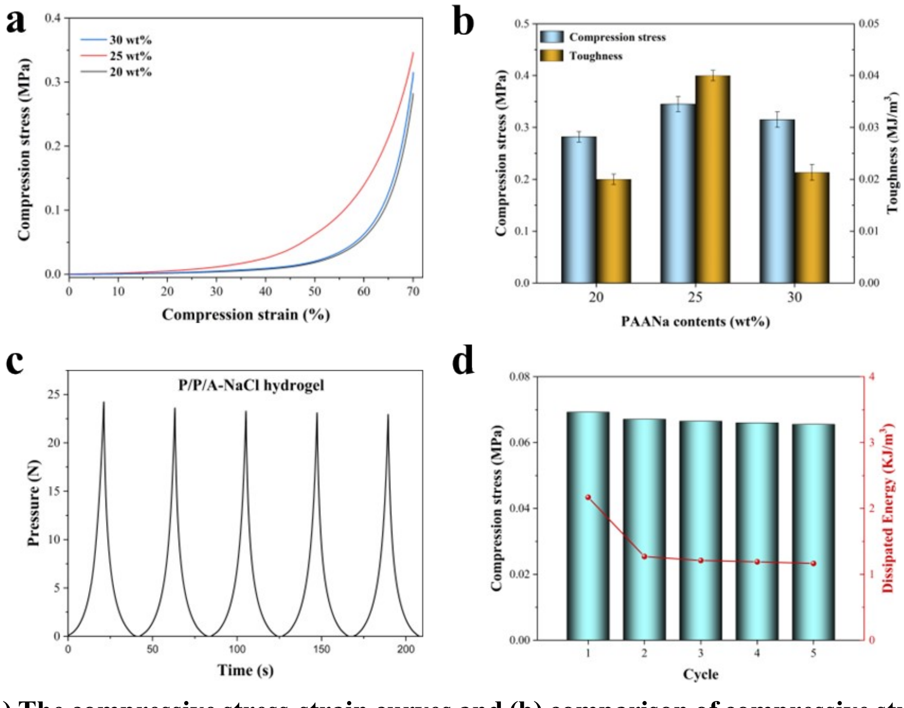

Fig. S8. (a) The compressive stress-strain curves and (b) comparison of compressive stress and toughness for P/P hydrogels with different PAANa contents. (c) The force-time curve and (d) compression stress value, as well as energy dissipation diagram of P/P/A-NaCl hydrogel for compression cycle.

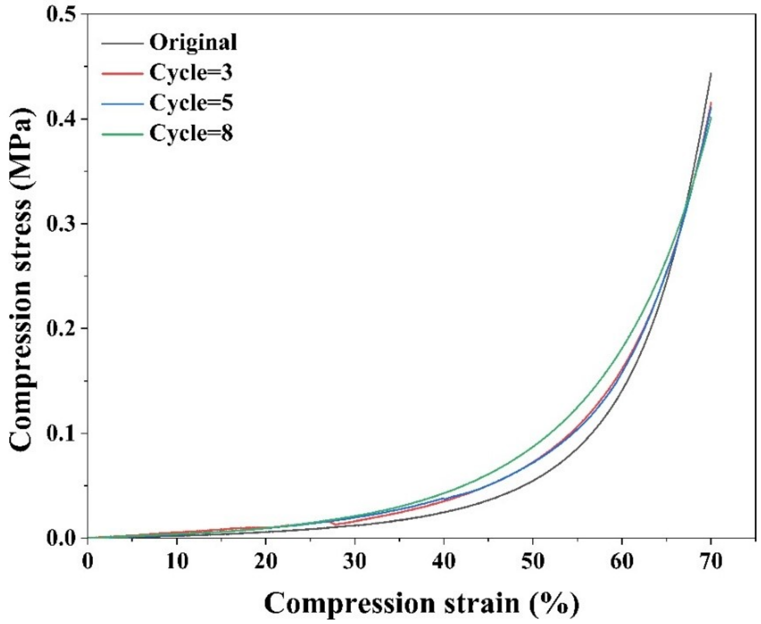

Fig. S9. The stress-strain curves of NaCl hydrogel after 3, 5, and 8 repeated hydration-dehydration cycles.

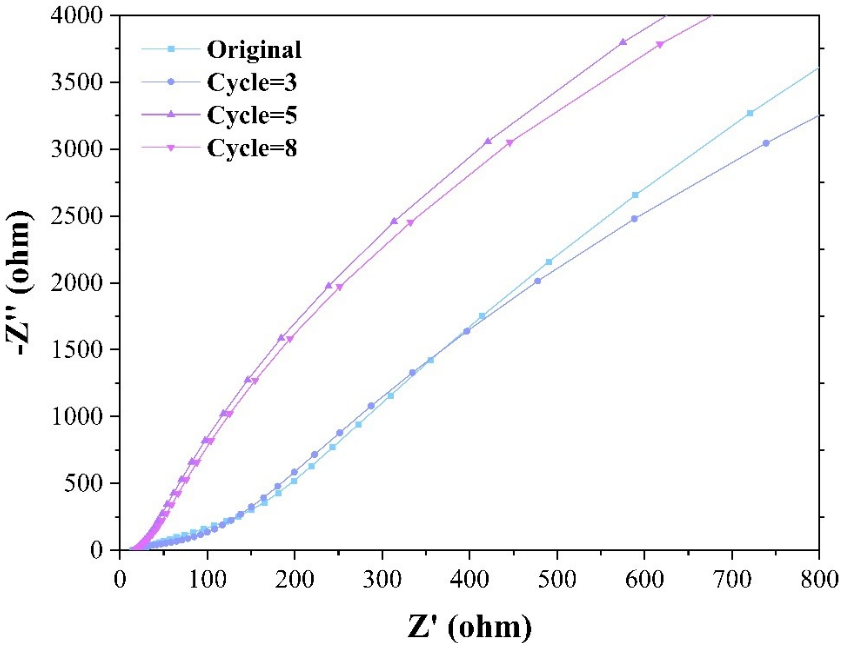

Fig. S10. The Nyquist curve of NaCl hydrogel after 3, 5, and 8 repeated hydration-dehydration cycles.

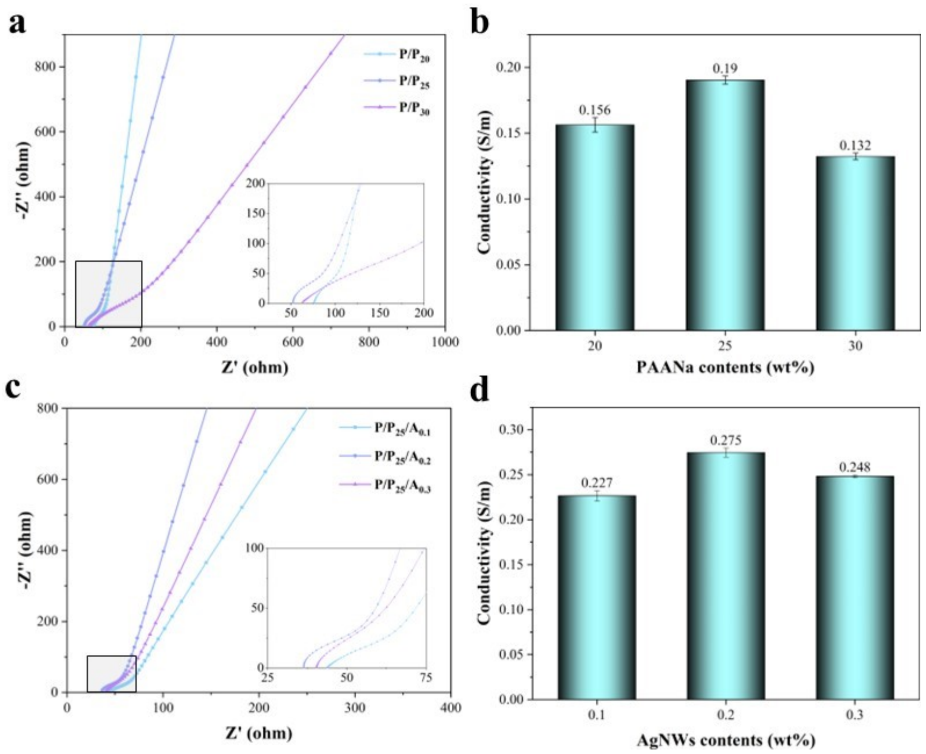

Fig. S11. (a) The Nyquist curve and (b) conductivity comparison diagram of P/P hydrogels with different PAANa contents. (c) The Nyquist curve and (d) conductivity comparison diagram of P/P/A hydrogel with different AgNWs contents.

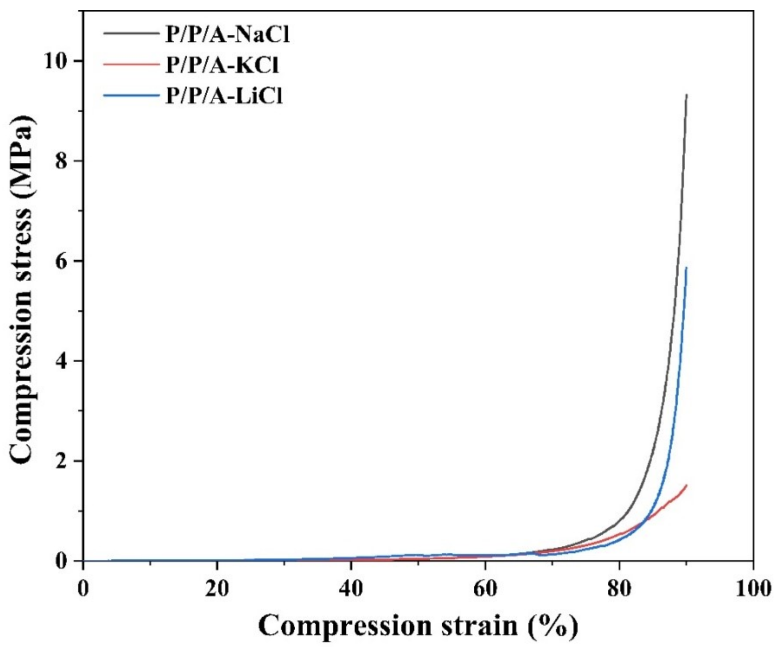

Fig. S12.The stress-strain curves of P/P/A hydrogels after being treated with NaCl, KCl and LiCl solutions, respectively.

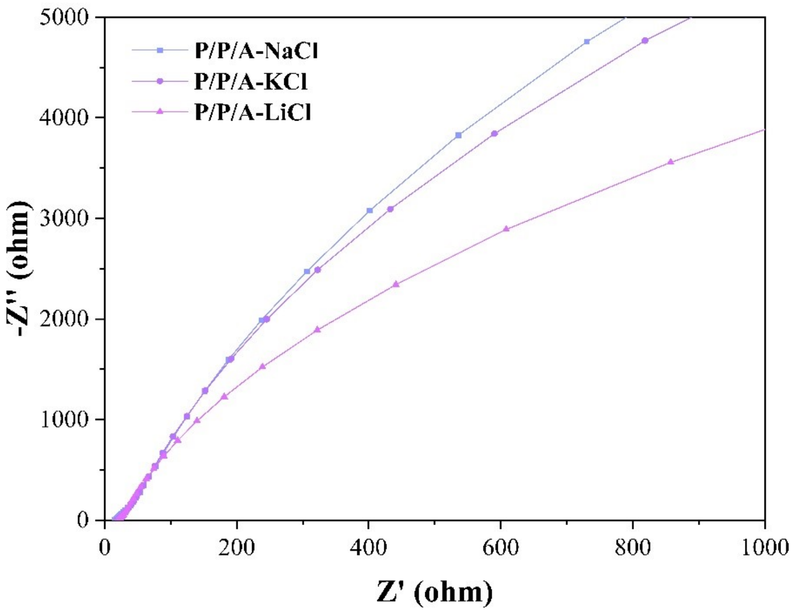

Fig. S13. The Nyquist curves of P/P/A hydrogels after treatment with NaCl, KCl and LiCl solutions respectively.

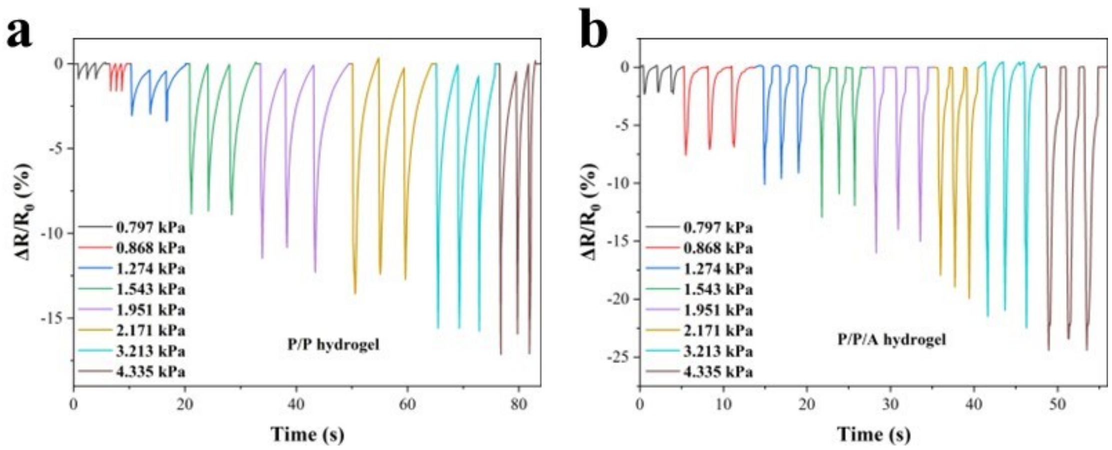

Fig. S14. (a) Real-time $\Delta R/R_0$ values of P/P hydrogel sensors at different pressures change. (b) Real-time $\Delta R/R_0$ values of P/P/A hydrogel sensors at different pressures change.

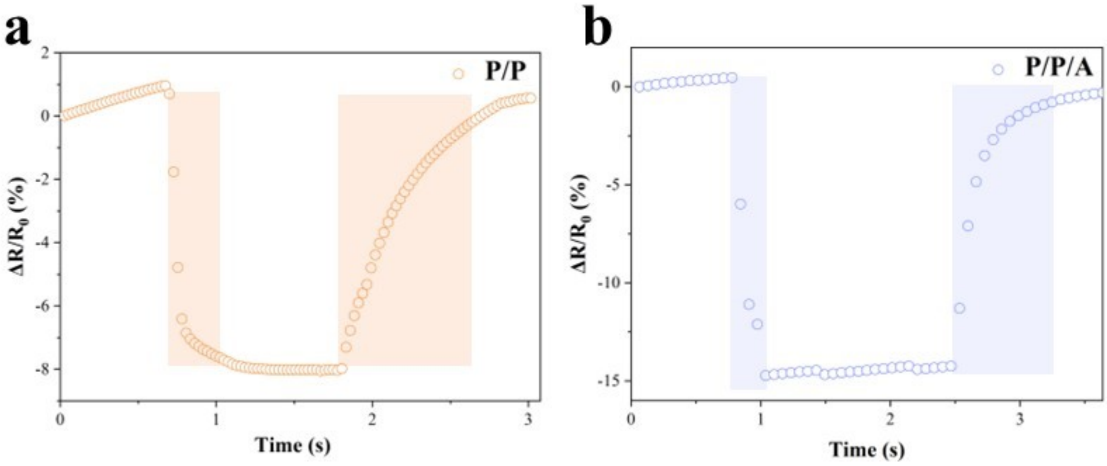

Fig. S15. (a) Response speed and recovery speed of P/P hydrogel sensors under pressure of 2.171kPa; (b) Response speed and recovery speed of P/P/A hydrogel sensors under pressure of 2.171kPa.

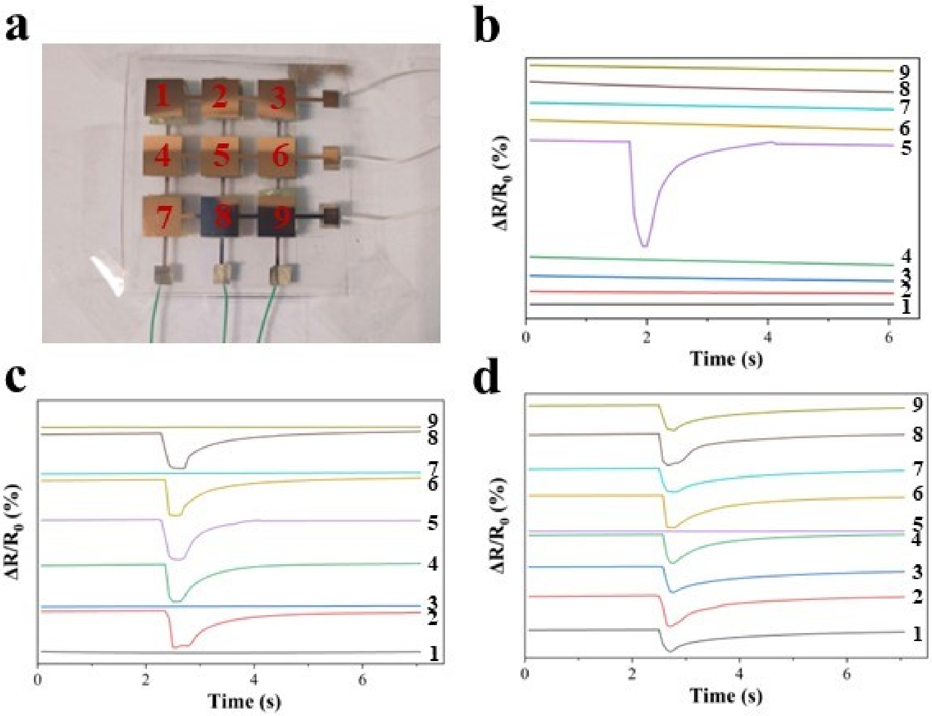

Fig. S16. (a) Optical photo of 3x3 array sensor. Place (b) 20g, (c) 200g and (d) tape in the array sensor corresponding to the real-time $\Delta R/R_0$ values.

Table S1. The Porosity characteristics of different composite hydrogels.

Sample	S_{BET} (m^2 g^{-1})	Average pore size (nm)
P/P	20.882	3.369
P/P/A	20.896	3.404
P/P/A-NaCl	32.925	3.660

Table S2. This work compares the properties of hydrogels with those in other literatures.

Materials	Fracture Stress	Conductivity	Sensitivity	Reference
PVA/PAANa/AgNWs	435 kPa	0.647 S m^{-1}	0.19	This work
Fibroin/Polyacrylamide	120 kPa	2.4 S cm^{-1}	-	R1
Poly(methyl methacrylate)	5 kPa	1.5 S m^{-1}	-	R2
PVA/Sodium alginate	118.8 kPa	0.256 S m^{-1}	0.39	R3
PVA/AgNWs	900 kPa	1.85 S m^{-1}	0.1	R4

References

[R1] G. Sun, et. al. “Ca^{2+}/ethanol driven in-situ integration of tough, antifreezing and conductive silk fibroin/polyacrylamide hydrogels for wearable sensors and electronic skin.” Chemical Engineering Journal, 2024, 497, 154745.

[R2] Y. Yang, et. al. “Conductive Organohydrogels with Ultrastretchability, Antifreezing, Self-Healing, and Adhesive Properties for Motion Detection and Signal Transmission.” ACS Appl Mater Interfaces, 2019, 11, 3428-3437.

[R3] Zheng, et. al. “A Low-Cost Hydrogel Electrode for Multifunctional Sensing: Strain, Temperature, and Electrophysiology.” Biosensors, 2025, 15,177.

[R4] S. Azadi, et. al. “Biocompatible and Highly Stretchable PVA/AgNWs Hydrogel Strain Sensors for Human Motion Detection.” Advanced Materials Technologies, 2020, 5, 2000426.